Superfluid transport in quantum spin chains

Silas Hoffman, Daniel Loss, and Yaroslav Tserkovnyak²

Department of Physics, University of Basel, Klingelbergstrasse 82, CH-4056 Basel, Switzerland
Department of Physics and Astronomy, University of California, Los Angeles, California 90095, USA



(Received 26 October 2018; revised 7 January 2023; accepted 17 January 2023; published 2 February 2023)

Spin superfluids enable long-distance spin transport through classical ferromagnets by developing topologically stable magnetic textures. For small spins at low dimensions, however, the topological protection suffers from strong quantum fluctuations. We study the remanence of spin superfluidity inherited from the classical magnet by considering the two-terminal spin transport through a finite spin-1/2 magnetic chain with planar exchange. By fermionizing the system, we recast the spin-transport problem in terms of quasiparticle transmission through a superconducting region. We show that the topological underpinnings of a semiclassical spin superfluid relate to the topological superconductivity in the fermionic representation. In particular, we find an efficient spin transmission through the magnetic region of a characteristic resonant length, which can be related to the properties of the boundary Majorana zero modes.

DOI: 10.1103/PhysRevB.107.085403

I. INTRODUCTION

In magnetic insulating materials, spin transport is mediated via spin-wave excitations or magnons rather than electrons [1]. Because the excitations in ferromagnetic insulators are bosonic, magnons are capable of supporting Bose-Einstein condensates [2] and even spin superfluid transport [3–5].

For a quasi-one-dimensional easy-plane magnet, the magnetic order is topologically characterized by the winding number of the mapping from \mathbb{R}^1 to S^1 . When a spin bias is applied to the boundary of such a system, topological defects in the magnetic texture, which are characterized by nontrivial winding numbers, are nucleated [6]. The ensuing topological transport yields a long-range spin supercurrent [4,7] subject to thermal [8] or quantum [9] phase slips. Such a supercurrent is suppressed, however, when the topological protection is destroyed by applying a magnetic field greater than the in-plane anisotropy. A preferred (easy) axis within the plane, furthermore, can reduce the mobility of the topological texture [7].

In contrast to (semi)classical magnets, the elementary excitations in quantum spin chains exhibit strong quantum fluctuations. In particular, in the extreme case of the lowest spin 1/2, it is unclear to which extent the superfluid character of the winding dynamics is applicable and useful. Recent spin-caloritronic experiments on spin liquids have demonstrated that spin can be transported via quantum spin excitations by thermal biasing [10]. With these practical tools in hand, an important open question concerns the possibility of long-range collective spin flows in quantum spin chains.

In this paper, we consider two semi-infinite XY spin chains, which realize Fermi-liquid-like spin reservoirs (Fig. 1). They supply and drain spin currents from a central region, whose transport is examined with an eye on spin superfluidity. We control the spin ordering and, consequently, the transport properties of the central region by applying an out-of-plane

magnetic field, which, in the semiclassical view, would tune the superfluid density, and an axial anisotropy within the easy (xy) plane, which breaks rotational symmetry and would pin the condensate phase. When the spins are uniformly ordered by a sufficiently large magnetic field, transport of low-energy excitations between the reservoirs is exponentially suppressed with the length of the central region. A chain with an easyplane anisotropy and a sufficiently small applied magnetic field affords zero-energy excitations which are transported ballistically. Although the bulk spectrum is gapped when there is an easy-axis anisotropy in the xy plane, evanescent domain walls at the ends of the chain survive which contribute to the transport. This is explicated by performing a nonlocal transformation which maps the spin operators to fermions [11]. In the fermionic language, the localized domain walls correspond to Majorana end modes. Analogous to the effect Majoranas have on the charge transport in topological superconductors, these localized domain walls qualitatively affect the transport in anisotropic spin chains. Specifically, for a sufficiently long central region, zero-energy excitations carrying positive spin along the z axis are perfectly reflected off the central region carrying negative spin; this is the analog of a perfect Andreev reflection from a topological superconductor [12]. Furthermore, zero-energy excitations can be ballistically transported through the central region when it is a certain resonant length, defined below, tunable by an applied magnetic field. This corresponds to perfect conductance of a fermion through a topological superconductor of the same resonant length; we are unaware of a discussion of such an effect in the literature.

II. GROUND STATES AND DOMAIN-WALL EXCITATIONS

A simple model to illustrate quantum transport is an N-site spin-1/2 ferromagnetic chain with a planar exchange

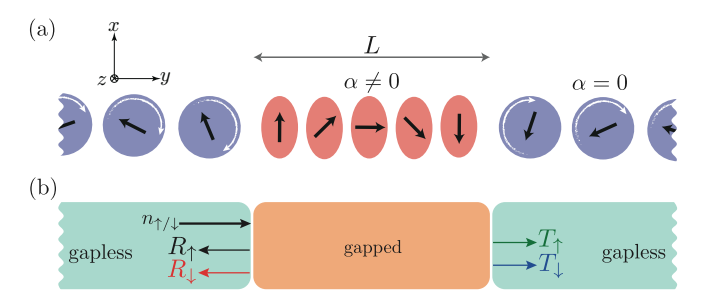


FIG. 1. (a) Schematic of our spin-1/2 chain setup. The left and right sides are semi-infinite spin chains (blue circles) wherein the spins are symmetrically coupled in the xy plane via an exchange coupling. The central region is of length L and has an in-plane anisotropy parameterized by α . (b) The left and right sides, absent of anisotropy, have a gapless spectrum, while the anisotropic central region is gapped. An incoming spin excitation, which is generically in a superposition of positive (a_{\uparrow}) and negative (a_{\downarrow}) spin collinear with the z axis, can be reflected (transmitted) as a spin up, R_{\uparrow} (T_{\uparrow}) , or spin down, R_{\downarrow} (T_{\downarrow}) , excitation.

coupling,

$$H = -J \sum_{i=1}^{N-1} \left[(1+\alpha)\sigma_i^x \sigma_{i+1}^x + (1-\alpha)\sigma_i^y \sigma_{i+1}^y \right] - h \sum_{i=1}^N \sigma_i^z,$$
(1)

where σ_i^{μ} for $\mu = x, y, z$ are the Pauli matrices acting on a spin at site i. Here, J is the exchange coupling between adjacent sites, α parameterizes the asymmetry in the xy plane, and h is the magnitude of an applied magnetic field along the z axis. Lengths are measured in units of the lattice spacing a. For the following discussion, we assume ferromagnetic exchange and so restrict the parameters as such, J > 0and $0 \le \alpha \le 1$ [13]. If there is no anisotropy, $\alpha = 0$, the Hamiltonian is rotationally symmetric about the z axis. For finite α , this symmetry is reduced to rotations by π . There is a quantum phase transition when the magnetic field is equal to the exchange, |h| = J. When |h| > J, the ground state is a nondegenerate with spins aligning according to the sign of the magnetic field. When |h| < J and $\alpha \neq 0$, the ground state is doubly degenerate. In the case of a quantum Ising chain absent of magnetic field, $\alpha = 1$ and h = 0, the two ground states correspond to the spins pointing homogenously parallel or antiparallel to the anisotropy axis. For the more general case, α < 1, at low fields, we can picture the magnetic moment along the (easy) anisotropy axis as an order parameter.

The spectrum is easily found upon performing a Jordan-Wigner transformation [11,14]. Defining a spinless fermionic creation (annihilation) operator at site j, $c_j^{\dagger} = \sigma_j^+ \mathcal{P}_j$ ($c_j = \sigma_j^- \mathcal{P}_j$) where $\sigma_j^{\pm} = (\sigma_j^x \pm i\sigma_j^y)/2$ and $\mathcal{P}_j = \prod_{l < j} (-\sigma_l^z)$. That is, c_j^{\dagger} or c_j polarize the spin at site j parallel or antiparallel to the z axis, respectively, while the sites before j are rotated by π around the z axis. When acting on the paramagnetic ground state, this corresponds to a spin flip at site j [Fig. 2(a)]. In the doubly degenerate phase, the action of these operators is most easily visualized in the Ising limit wherein the excitation is a domain wall at site j polarized parallel or antiparallel to the z axis [Fig. 2(b)], establishing a

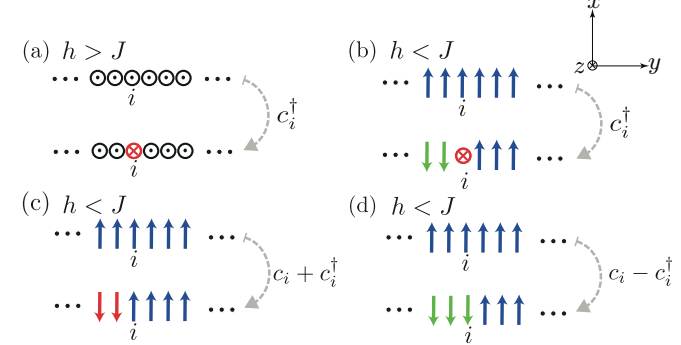


FIG. 2. The action of a fermionic creation operator, c_i^{\dagger} , (a) flips the spin at site i when |h| > J and (b) creates a domain wall pointing along the z axis when acting on the degenerate ground state, for |h| < J. (c) A superposition of $c_i + c_i^{\dagger}$ [(d) $c_i - c_i^{\dagger}$] rotates all sites before i by π around the z axis and the site i by π around the x (y) axis.

ferromagnetic analog of the Villain mode [15]. Although the spins are not collinear away from the Ising limit, $0 < \alpha < 1$, the action of c_j^{\dagger} and c_j on the ground state can similarly be regarded as the creation of a domain wall at site j.

Using these fermionic operators, Eq. (1) becomes

$$H = -\frac{J}{2} \sum_{i=1}^{N-1} (c_i^{\dagger} c_{i+1} + \alpha c_i^{\dagger} c_{i+1}^{\dagger} + \text{H.c.}) - h \sum_{i=1}^{N} (c_i^{\dagger} c_i - 1/2).$$
(2)

This is the Kitaev chain [16], describing a spinless metal (p-wave superconductor) for $\alpha=0$ ($\alpha\neq0$). The bulk excitations are known [17] and can be found in terms of the Fourier-transformed operators c_k and c_k^{\dagger} (see Appendix A). In the spin chain (metal) picture, c_k creates holes carrying $-\hbar$ spin quantized along the z axis (negative charge), while c_k^{\dagger} creates particles carrying \hbar spin (positive charge). Although conventionally these are regarded as delocalized particles or holes in the metallic picture, they can be equally well viewed as delocalized domain walls in the spin picture.

When the magnetic field is small, |h| < J, and the chain is absent of anisotropy, $\alpha = 0$, the spectrum consists of a partially filled gapless band [17]. There are two zero-energy modes with $\pm k_0 = \pm \cos^{-1}(h/J)$ defining the Fermi points. A zero-energy mode can be constructed as a superposition of c_{k_0} and $c_{k_0}^{\dagger} : a_{\downarrow} c_{k_0} + a_{\uparrow} c_{k_0}^{\dagger}$ with $a_{\uparrow} (a_{\downarrow})$ the spin-down (spin-up) amplitudes of the mode. Consider an excitation which has equal spin-up and spin-down amplitudes, $a_{\uparrow} = a_{\downarrow} e^{i\varphi} = e^{i\varphi/2}/\sqrt{2}$. Note that these are delocalized Majorana fermions as they are Hermitian. In the spin language, such an operator takes the form

$$(e^{i\varphi/2}c_{k_0} + e^{-i\varphi/2}c_{k_0}^{\dagger})/\sqrt{2}$$

$$= \sum_{j} \mathcal{P}_j \left[\cos(k_0 j + \varphi/2)\sigma_j^x + \sin(k_0 j + \varphi/2)\sigma_j^y\right]/\sqrt{2}.$$
(3)

In order to get a sense of the action of this operator, suppose it acts on a chain uniformly polarized along the x axis. The operator \mathcal{P}_j rotates the spins on the sites proceeding j by π around the z axis. The latter operator in Eq. (3) effectively rotates the

spin on site j by an angle $2(k_0j + \varphi/2)$. Consequently, the resultant state is a delocalized Bloch domain wall in which the spin at the center rotates clockwise with wavelength π/k_0 as it propagates along the chain [18]. Similarly, taking $k_0 \to -k_0$, the state is a domain wall rotating counterclockwise.

In the doubly degenerate ground state, |h| < J and $\alpha \neq 0$, the bulk spectrum is gapped. However, in a finite or semiinfinite chain, there exist zero-energy modes at the ends. In the fermionic language, these are the celebrated Majorana zero modes [16]. Together, these end modes form a nonlocal complex fermionic state which can be occupied or unoccupied, parametrizing the double degeneracy of the ground state. For the quantum Ising chain in the absence of magnetic field, $\alpha =$ 1 and h = 0, the zero-energy modes are localized to a single site: the modes at the left and right end are σ_1^x and $\mathcal{P}_N \sigma_N^y$, respectively [14]. The action of the product of these operators reverses the bulk Ising order. In the regime when h < 0 and $|h| \lesssim J$, the spin chain is largely polarized antiparallel to the z axis [19]. Focusing on low-energy excitations, we can pass from a discrete coordinate to a continuum, ℓ , measured with respect to the end of the chain. The mode at the left end is created by the operator $\int d\ell \sigma_{\ell}^{x} \mathcal{P}_{\ell}(e^{-\kappa^{+}\ell} - e^{-\kappa^{-}\ell})$, where $\kappa^+ = \alpha$ and $\kappa^- = (1 + h/J)/\alpha$. The mode at the right end is then created by $\int d\ell \sigma_\ell^y \mathcal{P}_\ell(e^{\kappa^+\ell} - e^{\kappa^-\ell})$ (see Appendix A). Although the ground states in a finite magnetic field are not uniformly ordered chains collinear with the x axis, the product of the zero-energy operators likewise reverses the bulk order between the two ground states. Analogous to the operators defined in Eq. (3) that create delocalized domain walls, the zero-energy operators create domain walls localized at the ends of the finite spin chain. When |h| > J, the system is trivially gapped and there exist no zero-energy bulk or localized modes.

III. TRANSPORT

To calculate the transport properties of a finite-size chain, consider a geometry in which the translational symmetry is broken: two semi-infinite isotropic spin chains ($\alpha = 0$) are connected to either side of a finite anisotropic chain ($\alpha \neq 0$ 0) of length L. See Fig. 1(a). The left and right isotropic sections of the chain are leads which provide a gapless source and drain of spin excitations, respectively, which probe the transport properties of the central gapped anisotropic region. Our setup is equivalent to a spinless normal metal|pwave superconductor normal metal junction through which charge transport is mapped to spin transport in the spin chain [Fig. 1(b)]. In general, the leads are held at a different magnetic field, h', from the magnetic field of the central region, h. Furthermore, after going from the discrete chain to the continuum limit, we include a δ -function potential of strength U separating the leads from the central region. Physically, this corresponds to a local magnetic field (scalar potential), on the scale of the lattice spacing, in the spin (electronic) picture. This barrier does not qualitatively affect our results but, for large U, makes the ratio of resonant and off-resonant transmission more dramatic [12].

In the following, we focus on the continuum limit of the system and proceed to calculate the scattering amplitudes in the fermionic description by matching the solutions at the

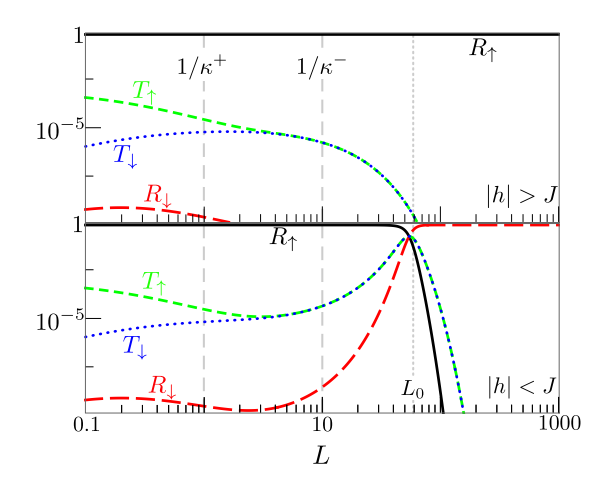


FIG. 3. The probability as a function of L of a zero-energy \hbar -spin excitation impinging on an ordered spin chain of length L to be reflected, R_{\uparrow} (R_{\downarrow}), with the same (opposite) spin or to be transmitted carrying positive (negative) spin, T_{\uparrow} (T_{\downarrow}). The plots are logarithmic on both axes and $\alpha = 1$, U/J = 10, and h'/J = -0.9. The upper panel is in the nondegenerate phase, h/J = -1.1, while the lower panel is in the degenerate phase, h/J = -0.9.

interfaces between the leads and central region. Consider a right-moving excitation in the left lead with energy E. In general, this can be a superposition of a particle carrying positive spin with wave vector $k^> = \sqrt{1 + (h' + E)/J}$ and a hole carrying negative spin with wave vector $k^< = \sqrt{1 + (h' - E)/J}$. The amplitude of the particle (hole) in the wave function is parameterized by a_{\uparrow} (a_{\downarrow}). Because spin along the z axis is not conserved in the central region, the incoming excitation can be reflected as a particle or a hole with probability R_{\uparrow} or R_{\downarrow} , respectively. The excitation can likewise be transmitted to the right lead as a particle (hole) with probability T_{\uparrow} (T_{\downarrow}).

Consider the regime near the topological phase transition, $\alpha^2 \gg |1+h/J|$, in which the spectrum is gapped by |h+J| at k=0. See Appendix A for a discussion of the spectrum. First, this limit allows us to contrast the transport properties in the degenerate, |h| < J, and nondegenerate, |h| > J, phases with equal gaps. Second, zero-energy in-gap states have two decay lengths which are well separated, $1/\kappa^+ = 1/\alpha \ll 1/\kappa^- = \alpha/(1+h/J)$, and allow us to obtain simple analytic solutions for the transport properties when $L \sim 1/\kappa^-$.

First, we consider a zero-energy excitation with spin along the z axis impinging on the central region, E=0 and $a_{\uparrow}=1$. When the length of the central region is short, $\kappa^+L\lesssim 1$, the transport properties of both degenerate and nondegenerate phases are characterized by an exponential suppression of the transmission and perfect reflection (Fig. 3). For $\kappa^+L\gg 1$, the two phases show a qualitative difference. In the nondegenerate phase, the transmittance remains exponentially suppressed and the reflection is perfect [Fig. 3 (upper panel)]. In the degenerate phase ($|h|\lesssim J$ and, to be specific, we take h<0), the transmission and reflection probabilities are

$$T_{\uparrow} = T_{\downarrow} = \mathrm{sech}^{2}[\kappa^{-}(L - L_{0})]/4,$$
 $R_{\uparrow} = e^{-2\kappa^{-}(L - L_{0})}\mathrm{sech}^{2}[\kappa^{-}(L - L_{0})]/4,$
 $R_{\downarrow} = e^{2\kappa^{-}(L - L_{0})}\mathrm{sech}^{2}[\kappa^{-}(L - L_{0})]/4,$ (4)

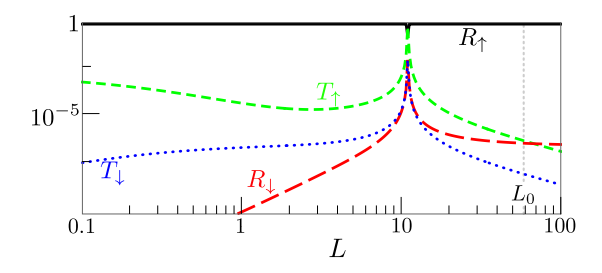


FIG. 4. Transmission probabilities, T_{\uparrow} and T_{\downarrow} , and reflection probabilities, R_{\uparrow} and R_{\downarrow} , as a function of L of an excitation with energy nearly at the gap edge, E=0.999(h+J), and positive spin, $a_{\uparrow}=1$ and $a_{\downarrow}=0$. The plots are logarithmic on both axes and we have taken $\alpha=1$, U/J=10, h/J=-0.9, and h'/J=-0.9.

where the resonant length

$$L_0 = \frac{\alpha}{1 + h/J} \ln \left[\frac{1 + h'/J + (\alpha/2 + U/J)^2}{\alpha \sqrt{1 + h'/J}} \right].$$
 (5)

When $1/\kappa^- \lesssim L < L_0$, the probability of transmission increases exponentially as the length of the central region increases [Eq. (4) and Fig. 3 (lower panel)]. At $L=L_0$, the probability to transmit a zero-energy excitation is locally maximized and $T_\uparrow = T_\downarrow = R_\uparrow = R_\downarrow = 1/4$ such that the excitation has equal probabilities of being reflected or transmitted as a spin up or spin down. Because $T_\uparrow = T_\downarrow$, no net spin is transferred between the leads. Beyond L_0 , the transmission is exponentially suppressed and the particle is favored to be reflected as a hole. That is, a spin of $2\hbar$ is perfectly injected into the anisotropic region. This is the spin-chain analog of a perfect Andreev reflection in one-dimensional topological superconductors [12].

The probability for an in-gap but finite energy, E, excitation to transmit through the central region is maximized at a length smaller than L_0 (Fig. 4). Furthermore, for an energy near the gap edge, $E \leq |h+J|$, the transmission probability, as a function of length, has the form of a Lorentzian (see Appendix B) rather than exponential as in Eq. (4). Because the mode interpolating between the leads is not at zero energy, the probability of transmission for a positive spin is different than for a negative spin, $T_{\uparrow} - T_{\downarrow} \approx (1 + h/J)/\alpha^2$, resulting in a net flow of spin. This restoration of long-distance transmission of spin is the remanence of classical spin supercurrent in the ordered quantum spin chain.

Rather than a spin polarized along the z axis, consider now a zero-energy incoming spin excitation which is equal parts spin up and spin down, e.g., in the sense of Eq. (3), scattering from the central region of the chain. In the electronic picture, this is equivalent to an incoming delocalized Majorana scattering from a p-wave superconductor. At zero energy, both the chain spectrum and the incoming excitation are particle-hole symmetric. Consequently, the outgoing state must also be particle-hole symmetric. Within the spin language, this implies that the probability of transmission (reflection) as spin up is equal to the probability of transmission (reflection) of spin down, $T_{\uparrow} = T_{\downarrow}$ ($R_{\uparrow} = R_{\downarrow}$). Although the peak in transmission remains at L_0 and is exponentially suppressed away from that length, the transmission strongly depends on φ [Eq. (3)]. Upon passing to the continuous coordinate, ℓ , the impinging spin

operator takes the form of Eq. (3), replacing i with ℓ . To avoid ambiguity in the definition of φ , we define the continuous coordinate so that $\ell=0$ corresponds to the interface between the left and central regions. At $L=L_0$, the transmission and reflection as a function of φ are

$$T_{\uparrow} = T_{\downarrow} = \frac{[2\sqrt{1 + h'/J}\cos(\varphi/2) + (\alpha + 2U)\sin(\varphi/2)]^{2}}{2[\alpha^{2} + 4\alpha U + 4(1 + h'/J + U^{2})]},$$

$$R_{\uparrow} = R_{\downarrow} = \frac{[(\alpha + 2U)\cos(\varphi/2) - 2\sqrt{1 + h'/J}\sin(\varphi/2)]^{2}}{2[\alpha^{2} + 4\alpha U + 4(1 + h'/J + U^{2})]},$$
(6)

respectively. In particular, when $\varphi = \varphi_0$ with

$$\varphi_0 = -2 \tan^{-1} \left[\frac{2\sqrt{1 + h'/J}}{(\alpha + 2U/J)^2)} \right] + \pi,$$
 (7)

the transmission is perfect, $T_{\uparrow} = T_{\downarrow} = 1/2$. Conversely, when $\varphi = \varphi_0 + \pi$, the excitation is perfectly reflected, $T_{\uparrow} = T_{\downarrow} = 0$.

These features in the transmission can be understood by the absence or presence and properties of the in-gap states. When |h| > J, transmission is suppressed for all L because there exist no in-gap states in the nondegenerate phase. In the degenerate phase, on the other hand, there exist in-gap evanescent end states which enhance transport. When $L \gg$ L_0 , the states do not overlap and there is no coherent transmission of the signal between the leads. When $L < L_0$, the end modes overlap and hybridize away from zero energy, thereby facilitating in-gap, finite-energy transport. Precisely at $L = L_0$, the end modes overlap but are stabilized at zero energy because they leak into the leads. Moreover, because the central region breaks gauge invariance when $\alpha \neq 0$, the transmission of an incoming Majorana [Eq. (3)] will depend on the phase difference between the particle and hole components. The resonance in transmission occurs when this phase for the incoming excitation matches the phase of the Majorana at the interface of the gapless and gapped regions.

Correspondingly, within the spin chain picture, the transmission and reflection can be viewed as domain-wall transport, e.g., in the sense of Eq. (3). For a sufficiently long central region, $L \gg L_0$, the incoming domain wall in the lead interacts with the domain wall localized at the interface and is reflected with opposite spin; remarkably, the presence of this localized domain wall serves as a perfect spin sink, independent of the effective barrier between the lead and the central region. At $L = L_0$, the domain walls are extended throughout the chain and support transport between the left and right regions. The spin analog of broken gauge invariance is an easy axis in the central region of our spin chain, e.g., the x axis in our system [Eq. (1)]. Although the orientation of the spin at the center of a domain wall can rotate in the gapless region, in the sense of Eq. (3), our results imply that the transmission through the central region depends on matching the easy axis and the domain-wall direction at the interface. In particular, when the spin configurations of the incoming domain wall and localized domain wall match, in the sense of $\varphi = \varphi_0$, we obtain a perfect conductance of these states through the central region and no signal at the right lead when their alignment is antiparallel, $\varphi = \varphi_0 + \pi$. Partial transmission can occur when, for instance, an equal parts superposition of two domain

walls with φ differing by π scatter from the central region. In particular, this is nicely illustrated when the central spin of the domain wall is collinear with the z axis [Eq. (4)], which can be written as a superposition of two domain walls, differing in relative phase by $\pm \pi$, with φ differing by π .

IV. DISCUSSION

We studied the low-energy transport through a quantum spin chain with an anisotropic planar exchange. We found that the most interesting features take place in the degenerate phase (|h| < J), which supports collective winding transport in the semiclassical spin perspective [4,7]. In the fermionic representation, this is the regime in which Majorana zero modes appear in long, isolated p-wave superconductors. We see that as a result, the most dramatic transport phenomena occur in this phase. In particular, fixing the transverse magnetic field, there is a length scale L_0 , which describes the onset of hybridization of the Majoranas in the presence of spin reservoirs. When $L \gg L_0$, the low-energy transmission is exponentially suppressed due to the spectral gap. When the length of the central region is reduced towards L_0 , the transmission kicks in exponentially at zero energy, where there is an equal transmission for both spin orientations along the z axis. Consequently, although there is no net spin flux, we expect a strong spin-current noise response at precisely this length. For $L < L_0$, the resonance in transmission moves to a finite energy, which supports net long-range spin transport and reflects the partial restoration of spin superfluidity [20]. The associated spin transport, or spin-current noise when $L = L_0$, may be measured by utilizing the spin Hall effect for spinto-charge conversion [21]. Moreover, the localized domain walls that are responsible for the underlying signal propagation could be imaged in real space, e.g., by a spin-polarized scanning tunneling microscopy or nitrogen-vacancy quantum sensors, although a detailed investigation of the key signatures associated with nonlocal spin transport is beyond our scope here.

In order to consider the effects of a disorder, suppose that the chain is made up of several segments, each with a random in-plane anisotropy. Adjacent regions whose anisotropies differ by an angle ϕ are connected by superconducting weak links as in a Kitaev chain [16]. Such a topological Josephson junction can support in-gap evanescent states whose energy is proportional to $\sin \phi$, where ϕ corresponds to *half* of the difference in the condensate phase across the junction. Hybridization of these localized states can form an in-gap band capable of supporting spin excitations [22]. In other words, disorder in the spin chain can globally smear the in-plane anisotropy on average, thereby restoring low-energy ballistic spin transport.

Throughout this manuscript, we have neglected additional out-of-plane exchange interactions, i.e., along the *z* axis in addition to exchange in the *xy* plane, between neighboring sites. It is known that such an *antiferromagnetic* exchange, corresponding to a repulsive interaction in the fermionic picture, can modify the order [23] and destroy the end states [24] for a sufficiently strong interaction. As a result, perfect Andreev reflection is destroyed and excitations are normally reflected at the interface with the anisotropic region even when

the magnetic field is smaller than the exchange [25]. Upon the inclusion of an out-of-plane *ferromagnetic* exchange interaction, on the other hand, which corresponds to an attractive interaction in the fermionic picture, perfect spin injection into the anisotropic region remains even for a strong out-of-plane exchange and can persist for large applied magnetic fields [25]. In future work, it may be interesting to investigate the length dependence of the associated spin transport [26].

ACKNOWLEDGMENTS

The authors acknowledge beneficial discussions with Victor Chua. This work was supported by the Swiss NSF, NCCR QSIT, and NSF under Grant No. DMR-2049979 (YT).

APPENDIX A: KITAEV HAMILTONIAN

The Kitaev Hamiltonian, given by Eq. (2) in the main text, can be Fourier transformed to momentum space taking the form $H = \frac{1}{2} \sum_k C_k^{\dagger} \mathcal{H} C_k$, where the sum is over k in the Brillouin zone and

$$\mathcal{H} = -(J\cos k + h)\eta_z - (\alpha J\sin k)\eta_y, \quad C_k^{\dagger} = [c_k^{\dagger}, c_{-k}]. \tag{A1}$$

Here, η_j are the Pauli matrices acting in Nambu space. In the following, we are interested in long wavelengths as compared to the lattice spacing, which is valid when |h| is comparable to J, so that the low-energy Hamiltonian is

$$\mathcal{H} = J[k^2 - (1 + h/J)]\eta_z - k\alpha J\eta_y, \tag{A2}$$

where we henceforth take h < 0. When $\alpha = 0$, the energies are $\pm J[k^2 - (1 + h/J)]$ for the respective eigenvectors $\varphi^+ = (1,0)$ and $\varphi^- = (0,1)$. The spectrum has two Fermi points, $\pm k \pm \sqrt{1 + h/J}$ [Fig. 5 (inset)]. If |h| > J|, the spectrum has a gap of |h + J| at k = 0. When $\alpha \neq 0$, the eigenvalues and eigenvectors are given by

$$E^{\pm}/J = \pm \sqrt{[k^2 - (1 + h/J)]^2 + \alpha^2 k^2},$$

$$\phi_k^{\pm} = \left[\frac{k^2 - (1 + h/J) + E^{\pm}/J}{-i\alpha k}, 1 \right],$$
(A3)

respectively.

For finite α , the spectrum E^{\pm} has a gap which closes at k = 0 when |h| = J, signaling a phase transition with |h| < J (|h| > J) supporting a degenerate (nondegenerate) ground state. There are two qualitatively different regimes of the spectrum: (1) when $2\alpha^2 > |1 + h/J|$ [Fig. 5 (black solid and red dashed curve)] and (2) when $2\alpha^2 < (1 + h/J)$ [Fig. 5 (green dotted curve)]. In the first case, there is one minimum in the spectrum at k = 0 with gap |h + J|. Near the phase transition when the energy is within the gap, $\alpha J \gg |h+J| > E$, all the wave vectors are purely imaginary, given by $\pm i\alpha$ and $\pm i\sqrt{(h+J)^2-E^2}/\alpha J$, i.e., there are no propagating solutions. When the energy is above the gap but still near the bottom of the band $(\alpha J \gg E > |h+J|)$, there are two propagating solutions, $\pm \sqrt{E^2 - (h+J)^2}/\alpha J$, and two totally imaginary wave vectors, $\pm i\alpha$. In the second case, there are two minima in the spectrum which are symmetric about k = 0 where there is a local maximum. Deep within the degenerate regime, $(1 + h/J) \gg \alpha^2$,

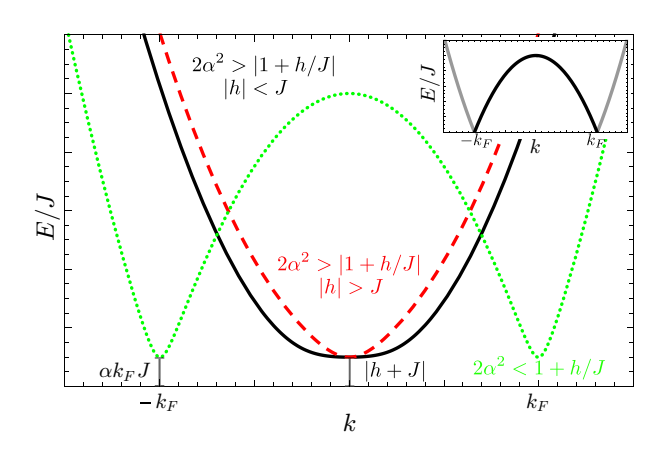


FIG. 5. The positive energy spectrum of the spin chain system with periodic boundary conditions in three regimes: (1) $2\alpha^2 > |1 + h/J|$ and |h| < J (black solid curve), (2) $2\alpha^2 > |1 + h/J|$ and |h| > J (red dashed curve), and (3) $2\alpha^2 < 1 + h/J$ (green dotted curve). Inset: The positive energy spectrum when $\alpha = 0$ and |h| < J. The excitations for $k < |k_F|(k > |k_F|)$ correspond to particles (holes).

the minima are at $\pm k_F$ with gap $\alpha k_F J$. When the energy is within the gap, $E < \alpha k_F J$, the four wave vectors are $k_F \pm i \sqrt{\alpha^2 - E^2/J(h+J)}$ and $-k_F \pm i \sqrt{\alpha^2 - E^2/J(h+J)}$; they oscillate with wave vector k_F and decay or grow exponentially according to their depth within the gap. Above the gap with $E < \sqrt{(h+J)^2 + J(h+J)\alpha^2}$, there are four propagating states with $k_F \pm \sqrt{E^2/J(h+J) - \alpha^2}$ and $-k_F \pm \sqrt{E^2/J(h+J) - \alpha^2}$, i.e., two solutions around each Fermi point. When $E > \sqrt{(h+J)^2 + J(h+J)\alpha^2}$, there are two

purely imaginary and two purely real solutions symmetric about k = 0.

In the gapped system, we expect the zero-energy states to be evanescent and consider the chain to be semi-infinite, passing to the continuum limit, with $\ell \geqslant 0$ being the coordinate along the chain. Near the phase transition, $|h| \approx J$, the wave vectors corresponding to solutions vanishing as $\ell \to \infty$ are $k^{\pm} = -i\kappa^{\pm}$ with $\kappa^{+} = \alpha$ and $\kappa^{-} = |1 + h/J|/\alpha$. The eigenvectors of these solutions are $\phi_{\kappa^{+}} = [1, 1]$ and $\phi_{\kappa^{-}} = [\operatorname{sgn}(1 + h/J), 1]$. Because the zero-energy wave function can only be made to vanish at $\ell = 0$ if the eigenvectors are parallel, such evanescent states are only present when |h| < J. Furthermore, because the particle and hole components are of equal weight, such a solution corresponds to a Majorana bound state up to an overall phase. As a general excitation can be written as $\Phi_k = \phi_k \cdot C_k = \int d\ell \phi_k \cdot C_\ell e^{-ik\ell}$, where $C_\ell^{\dagger} = [c_\ell^{\dagger}, c_\ell]$, the Majorana zero mode is

$$\Phi_M = \int d\ell (c_\ell + c_\ell^{\dagger}) (e^{-\kappa^+ \ell} - e^{-\kappa^- \ell}). \tag{A4}$$

APPENDIX B: TRANSPORT COEFFICIENTS

In general, the solutions for the transport coefficients are rather complicated. However, when $|1+h/J|\ll 1$, the separation in length scales allows us to obtain a simplified formula for these coefficients in two regimes: $\kappa^-L\ll 1$ and $\kappa^+L\gg 1$. Because we are interested in the long length behavior in the degenerate phase, we focus on the regime when $L\gg\kappa^+$ and |h|< J.

When the incoming excitation is at zero energy, E = 0, and polarized along z the transport coefficients are

$$t_{\uparrow} = 4i\alpha k_{F} e^{(-ik_{F} - \kappa^{-})L} \frac{[(\alpha + 2U/J)^{2} + (2k_{F})^{2}]a_{\downarrow} - (\alpha + 2ik_{F} + 2U/J)^{2}a_{\uparrow}}{[(\alpha + 2U/J)^{2} + (2k_{F})^{2}]^{2} e^{-2\kappa^{-}L} + (4\alpha k_{F})^{2}},$$

$$t_{\downarrow} = 4i\alpha k_{F} e^{(ik_{F} - \kappa^{-})L} \frac{(\alpha - 2ik_{F} + 2U/J)^{2}a_{\downarrow} - [(\alpha + 2U/J)^{2} + (2k_{F})^{2}]a_{\uparrow}}{[(\alpha + 2U/J)^{2} + (2k_{F})^{2}]^{2} e^{-2\kappa^{-}L} + (4\alpha k_{F})^{2}},$$

$$r_{\uparrow} = -\frac{[(\alpha - 2ik_{F} + 2U/J)(\alpha + 2ik_{F} + 2U/J)^{3}]a_{\uparrow} e^{-2\kappa^{-}L} + (4\alpha k_{F})^{2}a_{\downarrow}}{[(\alpha + 2U/J)^{2} + (2k_{F})^{2}]^{2} e^{-2\kappa^{-}L} + (4\alpha k_{F})^{2}},$$

$$r_{\downarrow} = -\frac{[(\alpha - 2ik_{F} + 2U/J)(\alpha + 2ik_{F} + 2U/J)^{3}]a_{\downarrow} e^{-2\kappa^{-}L} + (4\alpha k_{F})^{2}a_{\uparrow}}{[(\alpha + 2U/J)^{2} + (2k_{F})^{2}]^{2} e^{-2\kappa^{-}L} + (4\alpha k_{F})^{2}},$$
(B1)

where we have redefined $k_F = \sqrt{1 + h'/J}$ to be the Fermi points in the leads.

The complex conjugate square of these quantities are the transport probabilities in the main text: $R_{\uparrow} = |r_{\uparrow}|^2$, $R_{\downarrow} = |r_{\downarrow}|^2$, $T_{\uparrow} = |t_{\uparrow}|^2$, and $T_{\downarrow} = |t_{\downarrow}|^2$. One can show that the denominator of the transmission is minimized for the resonant length, L_0 [Eq. (5) in the main text], which is independent of the polarization of the incoming excitation.

When the magnitudes of the incoming spin-up and -down excitation are equal but differ in a phase φ [Eq. (3)],

$$|t_{\uparrow}| = |t_{\downarrow}| = \frac{\sqrt{24\alpha k_F} \sqrt{(\alpha + 2U/J)^2 + (2k_F)^2} [2k_F \cos(\varphi/2) + (\alpha + 2U/J)\sin(\varphi/2)] e^{\kappa^- L}}{[(\alpha + 2U/J)^2 + (2k_F)^2]^2 + (4\alpha k_F)^2 e^{2\kappa^- L}}.$$
 (B2)

One can show that the transmission is maximized when

$$e^{i\varphi} = -\frac{\alpha - 2ik_F + 2U/J}{\alpha + 2ik_F + 2U/J},\tag{B3}$$

which is equivalent to Eq. (7) in the main text. Using the condition $\alpha^2 \gg |1 + h/J|$, when U = 0 ($U/J \gg \alpha$), we find $\varphi \approx 0$ ($\varphi \approx \pi$).

We now consider the transmission coefficients of an excitation with positive energy within the gap, 0 < E < h + J, and polarized along z scattering off the central region. As the energy approaches the band gap, $E \to h + J$, the transport coefficients are

$$t_{\uparrow} = e^{-ik_{F}L} \frac{w_{\uparrow}}{u + vL}, \quad t_{\downarrow} = e^{-ik_{F}L} \frac{w_{\downarrow}}{u + vL},$$

$$w_{\uparrow} = 4\alpha k_{F}J^{3}[-i\alpha J(a_{\uparrow} - a_{\downarrow}) + 2k_{F}J(a_{\uparrow} + a_{\downarrow}) - 2iU(a_{\uparrow} - a_{\downarrow})][\alpha^{3}J^{2} + 2\alpha^{2}J(ik_{F}J + U) + 4(h + J)(ik_{F}J + U)],$$

$$w_{\downarrow} = 4\alpha^{2}k_{F}J^{3}[-i\alpha J(a_{\uparrow} - a_{\downarrow}) + 2k_{F}J(a_{\uparrow} + a_{\downarrow}) - 2iU(a_{\uparrow} - a_{\downarrow})][\alpha^{2}J^{2} - 2J(h + J) + 2\alpha J(-ik_{F}J + U)],$$

$$u = \{\alpha^{2}J^{2} + 4\alpha J(ik_{F}J + U) + 4[(k_{F}J)^{2} + U^{2}]\}$$

$$\times \{\alpha^{4}J^{4} + 4\alpha^{3}J^{3}(-ik_{F}J + U) + 8J(h + J)[(k_{F}J)^{2} + U^{2}] + \alpha^{2}J^{2}[4(k_{F}J)^{2} - 2J(h + J) + 4U^{2}]\},$$

$$v = -\alpha J(h + J)\{\alpha^{2}J^{2} + 4\alpha J(ik_{F}J + U) + 4[(k_{F}J)^{2} + U^{2}]\}^{2}.$$
(B4)

Note that to obtain these expressions, we have assumed that the energy of the excitation is much smaller than h' + J.

At the band edge, $|t_{\uparrow}|^2$ and $|t_{\downarrow}|^2$ are Lorentzian functions of L whose prefactor, center, and width are complicated functions of the system parameters. To further simplify the expressions, consider the case of when the excitation in the left lead carries \hbar spin, $a_{\uparrow} = 1$ and $a_{\downarrow} = 0$. When $U \gg |h|$, J and making use of the limit $\alpha \gg (1 + h/J)$, we find

$$|t_{\uparrow}|^{2} = \frac{\left[\alpha^{2}J + 2(h+J)\right]^{2}}{4\left[\alpha^{2}J + (h+J)\right]^{2} + \left[\frac{(h+J)U^{2}}{k_{F}J^{2}}\right]^{2}\left[L - \frac{\alpha^{2}J + 2(h+J)}{\alpha(h+J)}\right]^{2}},$$

$$|t_{\downarrow}|^{2} = \frac{\alpha^{4}J^{2}}{4\left[\alpha^{2}J + (h+J)\right]^{2} + \left[\frac{(h+J)U^{2}}{k_{F}J^{2}}\right]^{2}\left[L - \frac{\alpha^{2}J + 2(h+J)}{\alpha(h+J)}\right]^{2}}.$$
(B5)

When $L = [\alpha^2 J + 2(h+J)]/\alpha(h+J)$, the transmission probabilities are maximized. Likewise, the net spin current, $|t_{\uparrow}|^2 - |t_{\downarrow}|^2$, is maximized to be $(1 + h/J)/[\alpha^2 + (1 + h/J)] \approx (1 + h/J)/\alpha^2$. We plot the probabilities for reflection and transmission in Fig. 4. Notice that the excitation is normally reflected for nearly all values of L, except a small range in which the tunneling is peaked.

- [1] A. Khitun, M. Bao, and K. L. Wang, IEEE Trans. Magn. 44, 2141 (2008); F. Meier and D. Loss, Phys. Rev. Lett. 90, 167204 (2003).
- [2] T. Nikuni, M. Oshikawa, A. Oosawa, and H. Tanaka, Phys. Rev. Lett. 84, 5868 (2000); A. Oosawa, M. Ishii, and H. Tanaka, J. Phys.: Condens. Matter 11, 265 (1999); T. Radu, H. Wilhelm, V. Yushankhai, D. Kovrizhin, R. Coldea, Z. Tylczynski, T. Lühmann, and F. Steglich, Phys. Rev. Lett. 95, 127202 (2005); S. Demokritov, V. Demidov, O. Dzyapko, G. Melkov, A. Serga, B. Hillebrands, and A. Slavin, Nature (London) 443, 430 (2006); K. Nakata, K. A. van Hoogdalem, P. Simon, and D. Loss, Phys. Rev. B 90, 144419 (2014); K. Nakata, P. Simon, and D. Loss, J. Phys. D 50, 114004 (2017).
- [3] E. Sonin, J. Expt. Theor. Phys 47, 1091 (1978); Adv. Phys. 59, 181 (2010); J. König, M. C. Bønsager, and A. H. MacDonald, Phys. Rev. Lett. 87, 187202 (2001); S. A. Bender, R. A. Duine, and Y. Tserkovnyak, *ibid.* 108, 246601 (2012); H. Chen, A. D. Kent, A. H. MacDonald, and I. Sodemann, Phys. Rev. B 90, 220401(R) (2014); W. Chen and M. Sigrist, *ibid.* 89, 024511 (2014); Phys. Rev. Lett. 114, 157203 (2015).
- [4] S. Takei and Y. Tserkovnyak, Phys. Rev. Lett. 112, 227201 (2014).
- [5] S. Takei, B. I. Halperin, A. Yacoby, and Y. Tserkovnyak, Phys. Rev. B 90, 094408 (2014).
- [6] S. K. Kim and Y. Tserkovnyak, Phys. Rev. B 94, 220404(R) (2016).
- [7] S. K. Kim, S. Takei, and Y. Tserkovnyak, Phys. Rev. B 92, 220409(R) (2015).

- [8] S. K. Kim, S. Takei, and Y. Tserkovnyak, Phys. Rev. B **93**, 020402(R) (2016).
- [9] S. K. Kim and Y. Tserkovnyak, Phys. Rev. Lett. 116, 127201 (2016).
- [10] D. Hirobe, M. Sato, T. Kawamata, Y. Shiomi, K.-I. Uchida, R. Iguchi, Y. Koike, S. Maekawa, and E. Saitoh, Nat. Phys. 13, 30 (2017).
- [11] E. Lieb, T. Schultz, and D. Mattis, Ann. Phys. 16, 407 (1961).
- [12] K. T. Law, P. A. Lee, and T. K. Ng, Phys. Rev. Lett. 103, 237001 (2009).
- [13] In the case of an antiferromagnet exchange, J<0, the analysis formally remains the same with $k\to k+\pi$.
- [14] Y. Tserkovnyak and D. Loss, Phys. Rev. A 84, 032333 (2011).
- [15] H.-B. Braun and D. Loss, Intl. J. Mod. Phys. B 10, 219 (1996).
- [16] A. Y. Kitaev, Phys. Usp. 44, 131 (2001).
- [17] J. Alicea, Y. Oreg, G. Refael, F. von Oppen, and M. P. A. Fisher, Nat. Phys. 7, 412 (2011).
- [18] V. Popkov, D. Karevski, and G. M. Schütz, Phys. Rev. E 88, 062118 (2013); V. Popkov and C. Presilla, Phys. Rev. A 93, 022111 (2016); V. Popkov and G. M. Schütz, Phys. Rev. E 95, 042128 (2017); V. Popkov, C. Presilla, and J. Schmidt, Phys. Rev. A 95, 052131 (2017); T. Posske and M. Thorwart, Phys. Rev. Lett. 122, 097204 (2019).
- [19] The discussion follows identically when h > 0, upon exchanging spins parallel to the z axis and spins antiparallel to the z axis or, in the fermionic language, exchanging particles and holes and expanding around $k = \pi$ rather than k = 0.

- [20] H. Ochoa, R. Zarzuela, and Y. Tserkovnyak, Phys. Rev. B **98**, 054424 (2018).
- [21] E. Saitoh, M. Ueda, H. Miyajima, and G. Tatara, Appl. Phys. Lett. 88, 182509 (2006); J. Aftergood and S. Takei, Phys. Rev. Res. 2, 033439 (2020).
- [22] J. Wang and S. Chakravarty, arXiv:1808.04481.
- [23] D. Loss and D. L. Maslov, Phys. Rev. Lett. 74, 178 (1995).
- [24] S. Gangadharaiah, B. Braunecker, P. Simon, and D. Loss, Phys. Rev. Lett. **107**, 036801 (2011).
- [25] L. Fidkowski, J. Alicea, N. H. Lindner, R. M. Lutchyn, and M. P. A. Fisher, Phys. Rev. B 85, 245121 (2012).
- [26] P. P. Aseev, D. Loss, and J. Klinovaja, Phys. Rev. B 98, 045416 (2018).